

# An Enzyme-Free Glucose Electrochemical Sensor for Detection of the Glucose in Serum Based on Nickel Nanoparticle/Carbon Quantum Dots

Xiaoling Yang<sup>1,2</sup>, Zhihong Yan<sup>1</sup>, Ruihui Huang<sup>2</sup>, Jing Wang<sup>2</sup>, Yingde Cui<sup>3,\*</sup>, Yi Liu<sup>1,2,\*</sup>

<sup>1</sup> College of Pharmacy, Guangdong Pharmaceutical University, Guangdong, China.

<sup>2</sup> School of pharmaceutical and chemical engineering, Guangdong Pharmaceutical University, Guangdong, China

<sup>3</sup> Guangzhou Vocational College of Science and Technology, Guangzhou, Guangdong 510550, China.

\*E-mail: [13602880087@139.com](mailto:13602880087@139.com), [1499088964@qq.com](mailto:1499088964@qq.com)

Received: 9 January 2021 / Accepted: 24 February 2021 / Published: 31 March 2021

---

A sensitive enzyme-free glucose electrochemical sensor was developed by continuous cyclic voltammetry. In this system, the carbon quantum dots are a kind of green environmental protection materials and the nickel nanoparticle is excellent electrocatalysts. The proposed sensor based on the above two kinds of materials was successfully applied to determine glucose in serum. The developed sensor exhibition wider response range (0.005~8.0mM) and possessed lower detection limit (0.98 $\mu$ M). Moreover, as-prepared biosensor exhibited prominent selectivity, stability and reproducibility and it was used for the determination of glucose in serum with satisfactory results.

---

Glucose sensor; Nickel nanoparticles; Carbon quantum dots; Enzyme-free

## 1. INTRODUCTION

Diabetes is a metabolic disease, mainly caused by insulin secretion defects or abnormal insulin action. The kidneys, cardiovascular and nervous systems of diabetic patients are easily damaged, leading to dysfunction or failure. Therefore, the detection of blood sugar is very important. Glucose sensors have important application value in clinical diagnosis and most of them have been commercialized [1-3]. Nowadays, glucose sensors are mainly divided into two categories: enzyme sensors and enzyme-free sensors [4-10]. The enzyme-free glucose sensor has attracted much attention because of its high stability and avoiding enzyme denaturation [11, 12].

Nickel nanoparticles (Ni NPs) are considered to be the most ideal electrochemical catalyst materials for glucose, there are many reports on nickel based materials [13-17]. The electrocatalytic

oxidation mechanism of glucose is well known, and related literature has been reported [18-20]. Ni NPs was widely used in electrocatalysis due to its good stability and excellent conductivity [21-23].

Carbon quantum dots (CQDs) is a new type of carbon-based material with excellent optical and chemical properties and have received widespread attention [24, 25]. So far, CQDs has been applied to bioimaging [26, 27], biosensing [28, 29], and other fields. Like other carbon materials (graphene oxide and carbon nanotubes), CQDs are also used in electrocatalysis [30-32].

In this study, an enzyme-free glucose electrochemical sensor was fabricated based on the Ni NPs and CQDs by simple continuous cyclic voltammetry. CQDs using pine leaf chlorophyll as carbon source were synthesized by the classical hydrothermal method. In the synergistic effect of nickel nanoparticles and carbon quantum dots, the sensor showed excellent catalytic activity for glucose. The corresponding electrocatalytic mechanism is described in the paper.

### 2.1 Reagents

Citric acid (CA), mercaptoethylamine and nickel chloride were purchased from Shanghai Maclean Biochemical Co., Ltd. (Shanghai, China). Glycine, lysine, glutamic acid, glucose and sucrose were purchased from Nine-Dinn Chemistry (Shanghai) Co., Ltd. (Shanghai, China). NaCl and KCl were purchased from Guangzhou Chemical Reagent Factory (Guangzhou, China). Ethanol and sodium hydroxide were purchased from Damao Chemical Reagent Factory (Tianjin, China). CaCO<sub>3</sub> was purchased from Shanghai Lingfeng Chemical Reagent Co., Ltd. (Shanghai, China). Deionized water was used throughout the experiment. All reagents are analytically pure.

### 2.2 Extraction of pine leaf chlorophyll

Pick fresh campus pine leaves, shred them to a length of 1~2 cm, weigh 7 g of the shredded leaves into a beaker, add acetone and 95% ethanol in a ratio of 2:1 to the beaker, add 1 g of CaCO<sub>3</sub>, and filter for half an hour after ultrasound, spare.

### 2.3 Preparation of CQDs

Add 5 g of citric acid, 10 g of pine leaf chlorophyll, and 2.403 g of  $\beta$ -mercaptoethylamine to a beaker filled with 100 mL of pure water and 20 mL of 95% ethanol. After mixing, divide the solution into 3 linings. Each lining is 40 mL, and the lining is loaded into a stainless steel reactor and reacted at 180 °C for 150 min. After the reaction, light yellow liquid carbon quantum dots are obtained. Put the above-mentioned carbon quantum dot liquid into a 1000 Da dialysis bag, place it in distilled water, and change the water every 5 h for 2 days. Obtain colorless transparent liquid carbon quantum dots. The dialysis carbon quantum dot solution was freeze-dried to obtain solid carbon quantum dots.

#### 2.4 Preparation of Ni/CQDs/GCE

Before each experiment, the GCE was polished with 0.05  $\mu\text{m}$  alumina powder and ultrasonically cleaned in ethanol and deionized water for 5 min. Apply 5  $\mu\text{L}$  of CQDs onto GCE and dry them with an infrared lamp to prepare CQDs/GCE. CQDs/GCE was placed in  $\text{NiCl}_2$  solution to make prepare Ni/CQDs/GCE by continuous cyclic voltammetry. Among them, the scanning range is from -0.05 V to -1.05 V, the scanning rate is  $50\text{mV s}^{-1}$  and finally Ni/CQDs/GCE was obtained. Using similar experimental steps, CQDs/GCE and Ni/GCE were prepared respectively.

#### 2.5 Characterization

The morphology of modified electrodes was studied by scanning electron microscopy (SEM) with a LEO1430 vs. (Carl Zeiss, Germany) instrument. The CHI660E electrochemical workstation was used to obtain Cyclic Voltammetry (CV) and Chronoamperometry data. The CHI660E electrochemical workstation used a three-electrode battery setup, with 0.1 M NaOH solution as the supporting electrolyte. A modified glassy carbon electrode (GCE) as the working electrode, a platinum sheet was used as the counter electrode, a silver-silver chloride electrode (Ag/AgCl) as the reference electrode. Chronoamperometry was performed under uniform instantaneous conditions. The sensor test was performed by adding glucose within a time interval of 30 s.

#### 3.1 Characterization of the CQDs and Ni/CQDs nanocomposites

The prepared CQDs and Ni/CQDs nanocomposites were characterized by SEM to study their surface morphology (Fig.1).

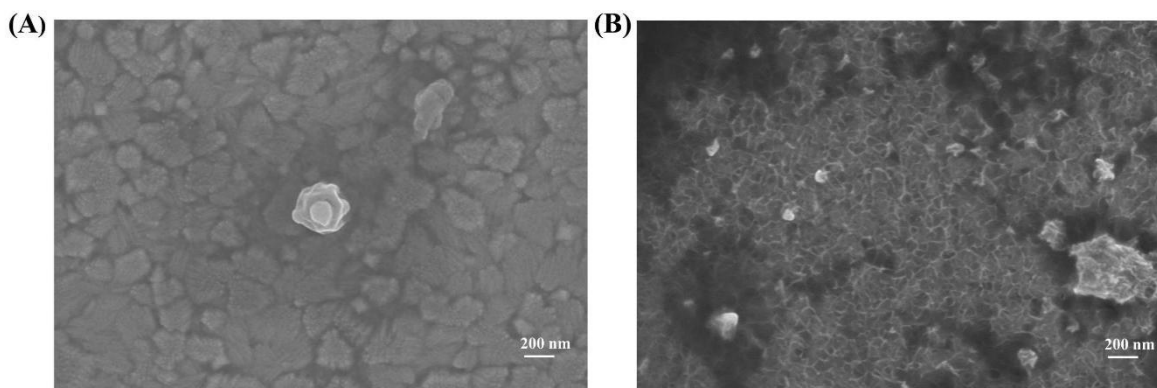


**Figure 1.** SEM images of CQDs (A) and Ni/CQDs nanocomposites (B).

The SEM image of CQDs synthesized by hydrothermal method using pine leaf chlorophyll as the raw material is shown in Fig.1A. It can be seen that the size of CQDs is about 2  $\mu\text{m}$ , has a spherical shape and a large specific surface area. Ni/CQDs/GCE was obtained by electrodeposition method, and its SEM image is shown in Fig.1B. Nano-nickel is uniformly and densely distributed on the surface of CQDs, and a relatively rough film is formed. Therefore, it can be concluded that the Ni/CQDs nanocomposite material was successfully obtained by a simple electrodeposition method and can be modified on the surface of the glassy carbon electrode.

### 3.2 Electrocatalytic oxidation of glucose at the Ni/CQDs/GCE

The electrocatalytic behavior of glucose on different modified electrodes was studied by cyclic voltammetry, and the results are shown in Fig.2. It can be seen from Fig.2B that during the glucose oxidation process of Ni/CQDs/GCE, a significant increase in anode current can be observed, and the oxidation potential shifted positively.

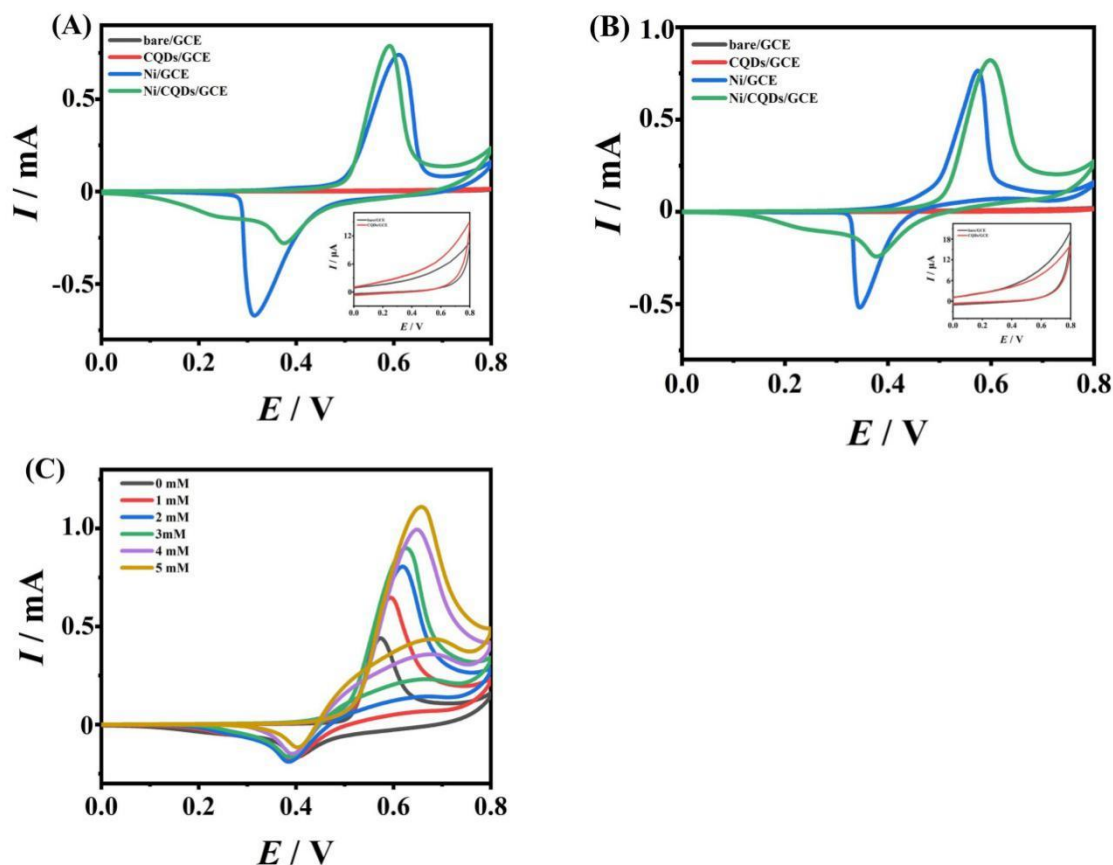
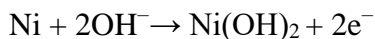


**Figure 2.** CV curves of bare/GCE, Ni/GCE, CQDs/GCE, Ni/CQDs/GCE without (A) or with 1 mM glucose (B) in 0.1 M NaOH solution. (C) CV curve of Ni/CQDs/GCE in 0.1 M NaOH solution containing different concentration of glucose with the scan rate is  $100\text{mV s}^{-1}$ .

These results may be due to the electrocatalytic oxidation of glucose adsorbed on  $\text{Ni}(\text{OH})_2$  surface. Oxidation of glucose occurs at a higher potential, which is mainly related to the chemical

reaction between nickel (II) and nickel (III) substances, and this process will lead to an increase in the anode peak current [33-35]. The chemical reaction process is as follows:



The cyclic voltammogram of the electrochemical catalysis behavior of glucose on Ni/CQDs/GCE was obtained from 0 to 5 mM glucose (Fig.2C). Obviously, the oxidation peak current value increases with the increase of glucose concentration. The results show that Ni/CQDs/GCE has good electrocatalytic oxidation behavior.

### 3.3 Optimization of conditions

#### 3.3.1 Scanning rate exploration

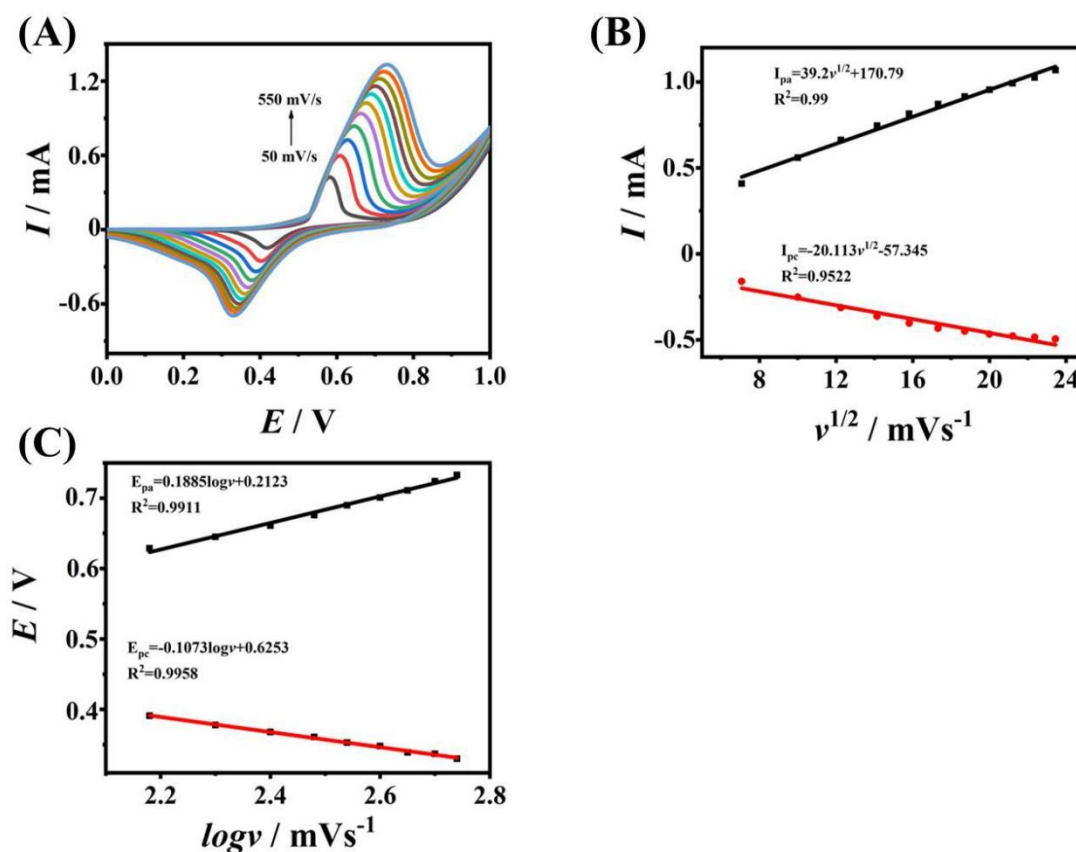


**Figure 3.** (A) CV curves of Ni/CQDs/GCE with 1 mM glucose in different scan rates. (B) Plot of square root of scan rate vs peak currents. (C) Plot of logarithm of scan rate vs peak potential.

In a 0.1 M NaOH solution containing 1 mM glucose, the kinetic process of glucose oxidation on Ni/CQDs/GCE was investigated by cyclic voltammetry at different scan rates (50~550  $\text{mV s}^{-1}$ ) (Fig.3A). As can be seen that the peak current of both anode and cathode increased with the increased

of scanning rate. Furthermore, the peak potentials of the anode and cathode had also changed. The peak potential of the anode moved to a high potential, and the peak potential of the cathode moved to a low potential. During the electrochemical reaction, the diffusion layer is dynamically restricted under high current density, which promotes the peak potential of the anode to move to a high potential [36]. As can be seen from Fig. 3B, there was a good linear relationship between the square root of the scan rate ( $v^{1/2}$ ) and the peak current. Fig. 3C showed the linear relationship between the logarithm of scanning rate ( $\log v$ ) and peak potential. These results indicate that the electrocatalytic oxidation process of glucose on Ni/CQDs/GCE is controlled by diffusion [37, 38].

### 3.3.2 Explore the impact of nickel chloride concentration

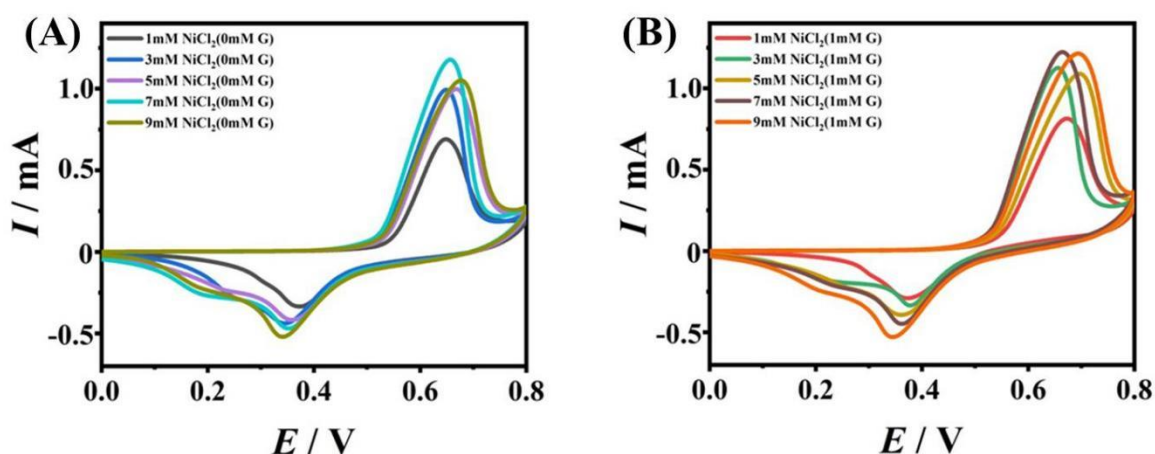


**Figure 4.** CV curve of Ni/CQDs/GCE in different concentrations nickel chloride without (A) or with 1 mM glucose (B) in 0.1 M NaOH solution with the scan rate is  $100\text{mV s}^{-1}$ .

**Table 1.** Differences in peak oxidation current values of Ni/CQDs/GCE obtained by electrochemical polymerization under different concentrations of nicks chloride before and after glucose addition.

Electrode	NiCl <sub>2</sub> (mM)	Glucose (mM)	I <sub>pa</sub> ( $\mu\text{A}$ )	$\Delta\text{Ipa}$ ( $\mu\text{A}$ )
Ni/CQDs/GCE	1	0	666	101
		1	767	
	3	0	944.3	139.7
		1	1084	
	5	0	950.7	47.7
		1	998.4	
	7	0	1121	41
		1	1162	
	9	0	990.8	112.2
		1	1103	

The preparation conditions were studied carefully to obtain the best sensing performance. Fig.4 confirmed the electrocatalytic function of Ni on glucose. It is of great significance to study the concentration of nickel chloride used to prepare Ni/CQDs/GCE. Ni/CQDs/GCE was obtained by continuous CV scanning in different concentrations of nickel chloride solution. In the absence of glucose (Fig.4A) and 1 mM glucose (Fig.4B), the electrocatalytic oxidation function of Ni on glucose was explored. It can be known from the difference in oxidation peak current value before and after glucose addition that when nickel chloride concentration was 3 mM, the oxidation current of glucose was the strongest (Table 1). Therefore, 3 mM nickel chloride was selected as the optimal concentration for the following test.

### 3.3.3 Explore the impact of scan cycles

At the same time, the effect of continuous CV scanning cycles of Ni/CQDs/GCE in 3 mM nickel chloride solution was also explored. The purpose is to find a suitable thickness to effectively catalyze the oxidation of glucose by controlling the number of cycles of electrochemical polymerization nickel. The results are shown in Fig.5 (A-B). As the number of cycles increases, the peak oxidation current increases and the potential shift positively. The thickness of the film formed by electrochemical polymerization gradually increases, which can promote the electrocatalytic oxidation of glucose. However, the comparison in Table 2 shows that when the number of cycles was 10, the difference in the oxidation peak current was the largest, indicating that the film on the surface of Ni/CQDs/GCE had reached the optimal thickness for the catalytic oxidation of glucose. Therefore, the sensitivity of Ni/CQDs/GCE in detecting glucose had been improved. When the thickness of the film is large, the obstacles to the electron transfer between the electrode and the solution increase. Hence, the film thickness obtained at the 10<sup>th</sup> cycle was selected as the optimal thickness.

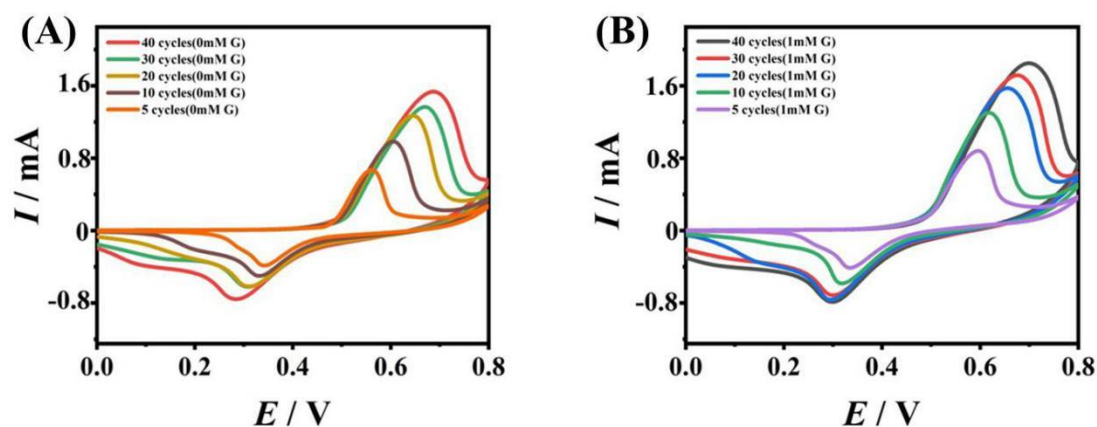


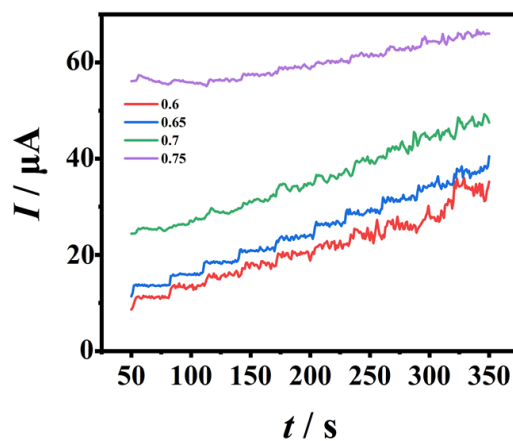
**Figure 5.** CV curve of Ni/CQDs/GCE in different number of scans without (A) or with 1 mM glucose (B) in 0.1 M NaOH solution with the scan rate is  $100\text{mV s}^{-1}$ .

**Table 2.** Differences in peak oxidation current values of Ni/CQDs/GCE with different cycles before and after glucose addition.

Electrode	Cycle number	Glucose (mM)	I <sub>pa</sub> (μA)	ΔI <sub>pa</sub> (μA)
Ni/CQDs/GCE	5	0	646.7	175.8
		1	822.5	
	10	0	938.5	255.5
		1	1194	
	20	0	1174	193
		1	1367	
	30	0	1235	212
		1	1447	
40	0	1273	207	
	1	1480		

### 3.4 Amperometric detection of glucose

Studies have shown that the sensing performance using current methods largely depends on the applied potential [42]. The amperometric response of Ni/CQDs/GCE under different applied potentials (+0.60~+0.75 V) was evaluated by adding 1 mM glucose to 0.1 M NaOH solution under stirring conditions. The current response curve obtained is shown in Fig.6.

**Figure 6.** Amperometric responses of Ni/CQDs/GCE to successive additions of 1mM glucose at the applied potentials of +0.60, +0.65, +0.70 and +0.75 V, respectively.

Obviously, it can be seen that under all the applied potentials studied, each time glucose was added, the current response increased gradually. It was worth noting that the highest sensitivity could be obtained at a potential of +0.65 V. Therefore, +0.65 V was chosen as the best potential for electrochemical detection of glucose.

Chronoamperometry was used to study the current response of Ni/CQDs/GCE to different concentrations of glucose at +0.65 V (Fig.7A). Different concentrations of glucose were added to 0.1 M NaOH solution every 30 s, and the solution was stirred to make the glucose dispersed evenly. When glucose was added to the solution, the current value increased rapidly and stabilized within 5 s, which indicated that Ni/CQDs/GCE had a rapid current response during the electrocatalytic oxidation of glucose. Uniform Ni NPs are loaded on the surface of the CQDs with a spherical structure, which provides many reaction sites for the electrocatalytic oxidation of glucose and promotes the rapid conversion of glucose to gluconolactone.

The linear relationship between current response and glucose concentration is shown in Fig. 7B. It can be seen that the current response increases in proportion to the increase in glucose concentration. The linear regression equation is  $I_{pa} = 5.8691c + 11.023$ , and the correlation coefficient is 0.9941. The results show that the linear range of Ni/CQDs/GCE for glucose detection is 0.005~8.0 mM, and the detection limit is 0.98  $\mu\text{M}$  (S/N=3).

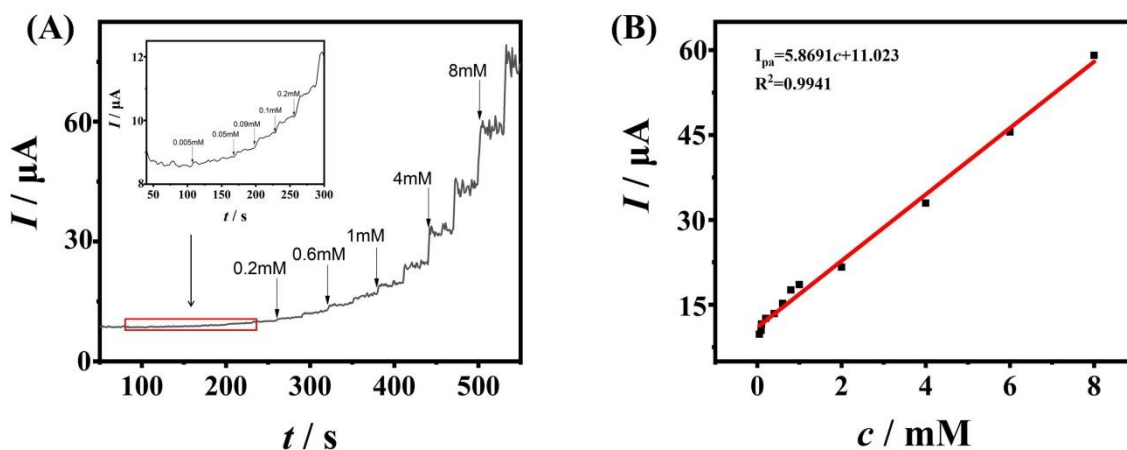


**Figure 7.** (A) Amperometric response of Ni/CQDs/GCE with adding glucose at time breaks of 30 s in 0.1M NaOH solution at +0.65 V. The inset is an enlarged view of the corresponding amperometric responses signal for glucose concentrations from 0.005 to 0.2mM. (B) Linear relationship between glucose concentration and response current.

### 3.5 Study of anti-interference, reproducibility and stability

The anti-interference ability of the glucose sensor is also a key factor, which is due to the presence of many interfering substances in the human blood environment, such as uric acid (UA), ascorbic acid (AA), glutamic acid (Glu), lysine (Lys) and NaCl, etc. Therefore, anti-interference experiments were carried out. Considering that the blood glucose concentration is 30 times that of

these interfering substances [39], after adding 1 mM glucose, 0.1 mM UA, AA, NaCl, KCl, Lys, Glu, Gly, and sucrose are added at +0.65 V (Fig.8). From the experimental results, it can be seen that a significant current change occurs after the addition of glucose. When the interfering substance is added, the current change is almost negligible, which shows that Ni/CQDs/GCE has excellent anti-interference ability when detecting glucose.

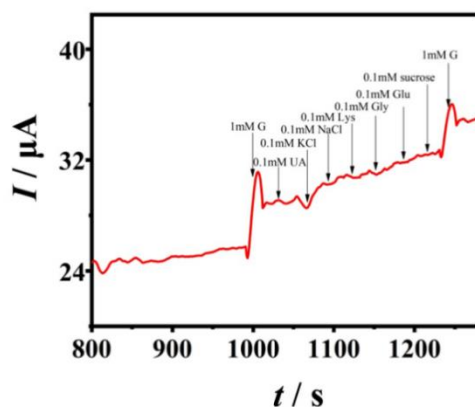


**Figure 8.** Anti-interference tests of the Ni/CQDs/GCE in 0.1 M NaOH solution at the applied potential of +0.65 V.

**Table 3.** Comparative performance data of nickel based enzyme-free sensors for glucose determination.

Electrode	Detection Limit ( $\mu\text{M}$ )	Linear range (mM)	Sensitivity ( $\mu\text{A mM}^{-1} \text{cm}^{-2}$ )	Reference
NiO/C microspheres	2	0.002~1.279	30.19	[40]
Ni(OH) <sub>2</sub> @PEDOT-rGO	0.6	0.002~7.1	346	[41]
Ni-MWNTs	0.89	0.0032~17.5	67.19	[42]
GQDs/CoNiAl-LDHs/CPE	6	0.01~1.4	48.717	[43]
NiAl-LDH/CC	0.22	0.001~0.329	14130	[44]
NiCo <sub>2</sub> O <sub>4</sub> @Ppy	0.22	0.01~20	3059	[45]
GCE-Graphene-Ni	0.1	0.01~1.15	2213	[46]
Chitosan-rGO-Ni NPs	4.1	up to 9	318.4	[47]
NiO-NPs@FTO	-	0.1~1.2	3.9	[48]
Ni/CQDs/GCE	0.98	0.005~8.0	11.74	This work

The reproducibility of Ni/CQDs/GCE was evaluated by measuring five independent sensors under the same conditions. It can be seen from the results that the relative standard deviation (RSD) of the current response value of five independent sensors measuring glucose is 2.37%, which means that Ni/CQDs/GCE has good reproducibility.

By exploring the long-term stability of Ni/CQDs/GCE, it can be used to evaluate its practical application. Store the prepared Ni/CQDs/GCE at room temperature to test its stability and regularly measure its current response to glucose. When the storage time is 7 days, Ni/CQDs/GCE maintains 93.8% of the initial current value, which has certain stability.

Table 3 compares the analytical performance of the prepared sensor and other nickel-based enzyme-free sensors. The comparison shows that Ni/CQDs/GCE has a wider linear range and lower detection limit when measuring glucose.

### 3.6 Measurement of chicken blood serum sample and human serum sample

The applicability of this glucose sensor was performed after determining the glucose concentration in real samples (chicken serum and human serum samples). Human serum samples came from the First Affiliated Hospital of Guangdong Pharmaceutical University.

**Table 4.** Determination of glucose in chicken blood serum sample by Ni/CQDs/GCE (n=3).

Analytes	Determined (mM)	Added (mM)	Found (mM)	Recovery (%)	RSD (%)
Glucose	2.18	2	4.08	97.60	3.61
		4	5.40	87.40	5.30
		8	9.38	92.10	4.80

RSD: Relative standard deviation of three measurements.

**Table 5.** Determination of glucose in human blood serum sample by Ni/CQDs/GCE (n=3).

Sample number	Measured by Ni/CQDs/GCE (mM)	Commercialized sensors (mM)	RSD (%)
1	3.71	3.83	2.20
2	4.78	4.97	2.80
3	4.49	4.20	4.70

Fresh chicken blood was collected from the local market. Using EDTA as an anticoagulant, the fresh chicken blood was centrifuged to obtain a chicken serum sample. The chicken serum sample was

diluted 100 times with 0.1 M NaOH solution, and then, at +0.65 V, the glucose recovery experiment in the chicken serum sample was carried out by the standard loading method using the current-time curve method. The results are shown in Table 4. At the same time, the electrochemical biosensor we prepared was also tested for human serum samples. The human serum sample was diluted 40 times with 0.1 M NaOH solution. The measurement results of the three human serum samples are listed in Table 5. These results show that the obtained sensor has good accuracy and precision, and proves that the prepared sensor has practical application value.

In summary, Ni NPs/CQDs nanocomposites were prepared by pine leaf chlorophyll, and a novel and sensitive enzyme-free glucose electrochemical sensor was prepared. Ni NPs were electrodeposited by simple continuous cyclic voltammetry based on the CQDs/GCE in 3 mM nickel chloride solution. The developed sensor showed good sensing performance for glucose monitoring. The linear range was 0.005~8 mM, the sensitivity was 11.74  $\mu\text{A mM}^{-1} \text{cm}^{-2}$ , and the detection limit was 0.98  $\mu\text{M}$  (S/N=3). The sensitivity, selectivity, repeatability, real sample analysis (real human serum sample and chicken serum sample), storage stability and repeatability of the prepared glucose sensor are all satisfactory. The preparation method of the enzyme-free glucose sensor is simple and environmentally friendly and effective. It provides a new idea for the preparation of enzyme-free glucose sensor.

This work was supported by the Guangdong Provincial Project (2016A010103039), Guangzhou Yuexiu District Science and Technology Plan Project (2017-WS-016), Guangdong Provincial Innovation and Entrepreneurship Training Program for College Students (S201910573034) is a key discipline jointly constructed by Guangdong and Zhongshan.

## References

1. D. Zhai, B. Liu, Y. Shi, L. Pan, Y. Wang, W. Li, R. Zhang and G. Yu, *ACS Nano*, 7(2013)3540-3546.
2. S.-K. Kim, C. Jeon, G.-H. Lee, J. Koo, S. H. Cho, S. Han, M.-H. Shin, J.-Y. Sim and S. K. Hahn, *ACS Appl. Mater. Interfaces*, 11(2019)37347-37356.
3. J. Hu, *Biosens. Bioelectron.*, 24(2009)1083-1089.
4. L. Ramasauskas, R. Meskys and D. Ratautas, *Biosens. Bioelectron.*, 164(2020)112338.
5. A. Samphao, P. Butmee, P. Saejueng, C. Pukahuta, L. Svorc and K. Kalcher, *J. Electroanal. Chem.*, 816(2018)179-188.
6. X. Wang, C.-y. Ge, K. Chen and Y. X. Zhang, *Electrochim. Acta*, 259(2018) 225-232.
7. N. Lu, C. Shao, X. Li, T. Shen, M. Zhang, F. Miao, P. Zhang, X. Zhang, K. Wang, Y. Zhang and Y. Liu, *RSC Adv.*, 4(2014)31056-31061.
8. K. Tian, M. Prestgard and A. Tiwari, *Mater. Sci. Eng., C*, 41(2014)100-118.
9. K. Ramachandran, T. Raj kumar, K. J. Babu and G. Gnana kumar, *Sci. Rep.*, 6(2016)36583.
10. E. Rafatmah and B. Hemmateenejad, *Sens. Actuators, B*, 304(2020)127335.

11. N. Yuhashi, M. Tomiyama, J. Okuda, S. Igarashi, K. Ikebukuro and K. Sode, *Biosens. Bioelectron.*, 20(2005)2145-2150.
12. C. Espro, S. Marini, D. Giusi, C. Ampelli and G. Neri, *J. Electroanal. Chem.*, 873(2020)114354.
13. A. Zeng, C. Jin, S.-J. Cho, H. O. Seo, Y. D. Kim, D. C. Lim, D. H. Kim, B. Hong and J.-H. Boo, *Mater. Res. Bull.*, 47(2012)2713-2716.
14. H. Karimi-Maleh, K. Cellat, K. Arikian, A. Savk, F. Karimi and F. Sen, *Mater. Chem. Phys.*, 250(2020)123042.
15. F. Wang, Y. Feng, S. He, L. Wang, M. Guo, Y. Cao, Y. Wang and Y. Yu, *Microchem. J.*, 155(2020)104748.
16. K. N. Brinda, G. Achar, J. G. Malecki, S. Budagumpi, D. H. Nagaraju, V. Suvina and R. G. Balakrishna, *Biosens. Bioelectron.*, 134(2019)24-28.
17. H. Wu, Y. Yu, W. Gao, A. Gao, A. M. Qasim, F. Zhang, J. Wang, K. Ding, G. Wu and P. K. Chu, *Sens. Actuators, B*, 251(2017)842-850.
18. A. A. Ensafi, N. Ahmadi and B. Rezaei, *Sens. Actuators, B*, 239(2017)807-815.
19. Z. Shen, W. Gao, P. Li, X. Wang, Q. Zheng, H. Wu, Y. Ma, W. Guan, S. Wu, Y. Yu and K. Ding, *Talanta*, 159(2016)194-199.
20. M. Yuan, X. Guo, N. Li, Q. Li, S. Wang, C.-S. Liu and H. Pang, *Sens. Actuators, B*, 297(2019)126809.
21. T. Liu, Y. Luo, J. Zhu, L. Kong, W. Wang and L. Tan, *Talanta*, 156-157(2016)134-140.
22. Y. Shu, Y. Yan, J. Chen, Q. Xu, H. Pang and X. Hu, *ACS Appl. Mater. Interfaces*, 9(2017)22342-22349.
23. X. Niu, M. Lan, H. Zhao and C. Chen, *Anal. Chem. (Washington, DC, U. S.)*, 2013, 85, 3561-3569.
24. Y. Guo and W. Zhao, *Coord. Chem. Rev.*, 387(2019)249-261.
25. P. Devi, P. Rajput, A. Thakur, K.-H. Kim and P. Kumar, *TrAC, Trends Anal. Chem.*, 114(2019)171-195.
26. Y. Guo, L. Zhang, S. Zhang, Y. Yang, X. Chen and M. Zhang, *Biosens. Bioelectron.*, 63(2015)61-71.
27. K. Jiang, S. Sun, L. Zhang, Y. Lu, A.G. Wu, C.Z. Cai and H.W. Lin, *Angew. Chem. Int. Ed.*, 54(2015)5360-5363.
28. Z. Tang, J. Yang, G. Li and Y. Hu, *Talanta*, 195(2019)550-557.
29. J. Deng, Q. Lu, Y. Hou, M. Liu, H. Li, Y. Zhang and S. Yao, *Anal. Chem. (Washington, DC, U. S.)*, 87(2015)2195-2203.
30. D. S. Su and G. Centi, *J. Energy Chem.*, 22(2013)151-173.
31. W.-S. Li, P.-X. Hou, C. Liu, D.-M. Sun, J. Yuan, S.-Y. Zhao, L.-C. Yin, H. Cong and H.-M. Cheng, *ACS Nano*, 7(2013)6831-6839.
32. V. C. Hoang, K. Dave and V. G. Gomes, *Nano Energy*, 66(2019)104093.
33. I. Danaee, M. Jafarian, F. Forouzandeh, F. Gobal and M. G. Mahjani, *Electrochim. Acta*, 53(2008)6602-6609.
34. M. Jafarian, F. Forouzandeh, I. Danaee, F. Gobal and M. G. Mahjani, *J. Solid State Electrochem.*, 13(2009)1171-1179.
35. P. R. Martins, M. A. Rocha, L. Angnes, H. E. Toma and K. Araki, *Electroanalysis*, 23(2011)2541-2548.
36. M. A. Al-Omar, A. H. Touny, F. A. Al-Odail and M. M. Saleh, *Electrocatalysis*, 8(2017)340-350.
37. J. Xu, T. Chen, X. Qiao, Q. Sheng, T. Yue and J. Zheng, *Colloids Surf., A*, 561(2019) 25-31.
38. M. Ma, W. Zhu, D. Zhao, Y. Ma, N. Hu, Y. Suo and J. Wang, *Sens. Actuators, B*, 278(2019)110-116.
39. X. Zhang, S. Sun, J. Lv, L. Tang, C. Kong, X. Song and Z. Yang, *J. Mater. Chem. A*, 2(2014)10073-10080.
40. Z. Cui, H. Yin and Q. Nie, *J. Alloys Compd.*, 632(2015) 402-407.

41. L. Sheng, Z. Li, A. Meng and Q. Xu, *Sens. Actuators, B*, 254(2018)1206-1215.
42. A. Sun, J. Zheng and Q. Sheng, *Electrochim. Acta*, 65(2012)64-69.
43. S. Samuei, J. Fakkar, Z. Rezvani, A. Shomali and B. Habibi, *Anal. Biochem.*, 521(2017)31-39.
44. B. Hai and Y. Zou, *Sens. Actuators, B*, 208(2015)143-150.
45. X. Duan, K. Liu, Y. Xu, M. Yuan, T. Gao and J. Wang, *Sens. Actuators, B*, 292(2019)121-128.
46. H. Wu, Y. Yu, W. Gao, A. Gao, A. M. Qasim, F. Zhang, J. Wang, K. Ding, G. Wu and P. K. Chu, *Sens. Actuators, B*, 251(2017)842-850.
47. S.-J. Li, N. Xia, X.-L. Lv, M.-M. Zhao, B.-Q. Yuan and H. Pang, *Sens. Actuators, B*, 190(2014)809-817.
48. S. Mishra, P. Yogi, P. R. Sagdeo and R. Kumar, *Nanoscale Res. Lett.*13(2018) 1-7.

© 2021 The Authors. Published by ESG ([www.electrochemsci.org](http://www.electrochemsci.org)). This article is an open access article distributed under the terms and conditions of the Creative Commons Attribution license (<http://creativecommons.org/licenses/by/4.0/>).